Electronic states of the $Cr_2O_3(0001)$ surface from *ab initio* embedded cluster calculations

1999 J. Phys.: Condens. Matter 11 7881

(http://iopscience.iop.org/0953-8984/11/40/319)

J. Phys.: Condens. Matter **11** (1999) 7881–7891. Printed in the UK PII: S0953-8984(99)02217-1

Electronic states of the $Cr_2O_3(0001)$ surface from *ab initio* embedded cluster calculations

J A Mejias†§, V Staemmler† and H-J Freund‡

† Lehrstuhl für Theoretische Chemie, Ruhr-Universität Bochum, Universitätsstrasse 150, D-44780 Bochum, Germany

‡ Fritz-Haber-Institut der Max-Planck Gesellschaft, Faradayweg 4-6, D-14195 Berlin, Germany

Received 2 March 1999

Abstract. The electronic structure of the $Cr_2O_3(0001)$ surface is studied by means of *ab initio* embedded cluster calculations. Charge distributions and local d–d excitations are analysed for different geometrical relaxations of the surface. In the ground state there is considerable delocalization of electrons from the oxygen 2p band into the partly occupied 3d AOs of the Cr cations at the surface such that their ionicity is reduced to Cr^{2+} as compared to Cr^{3+} in the bulk. The calculated d–d and charge transfer excitations agree very well with the prominent loss peaks observed experimentally by means of electron energy loss spectroscopy (EELS) at the $Cr_2O_3(0001)$ surface.

1. Introduction

Polar surfaces of ionic crystals, in particular of metal oxides, are thermodynamically unstable since the electrostatic surface energy diverges [1–3]. Such surfaces can, however, be stabilized by geometrical reconstructions and relaxations, as for instance observed for the NiO(111) surface [4, 5]. Alternatively, the response of the electrons to the surface dipole moment can cause modifications of the electronic structure at the surface as compared to the bulk, which in turn might also lead to a stabilization. Therefore, in order to understand the mechanism of stabilization of polar surfaces, both geometrical and electronic effects have to be considered.

One example of a polar metal oxide surface, studied recently in some detail, is the (0001) surface plane of Cr_2O_3 films grown on Cr(110) [6–8]. Bulk Cr_2O_3 has corundum-type structure, which consists of hexagonal closed packed (hcp) layers of oxygen atoms with the metal cations occupying two-thirds of the octahedral interstices. Figure 1 shows that along the (0001) direction flat oxygen layers alternate with buckled chromium layers. In order to preserve the stoichiometry, one of the three possible octahedral positions in the Cr layer is empty. This causes slight distortions in the hcp O layers which are completely planar but exhibit slightly differing O–O distances.

It is now well established, both theoretically [8, 9] and experimentally [7, 8], that the polar Cr-terminated $Cr_2O_3(0001)$ surface plane is stabilized by two effects. First, half of the chromium ions at the surface are removed. By this, the surface charge is reduced and the divergence of the electrostatic surface energy is avoided [1, 2]. SCF calculations [9] as well as molecular dynamics (MD) simulations [8] have shown that the Cr ions in site 2 (i.e., those ions

§ Present address: Facultad de ciencias experimentales, Universidad Pablo de Olavide, Carretera de Utrera Km 1, 41013 Sevilla, Spain.

0953-8984/99/407881+11$30.00

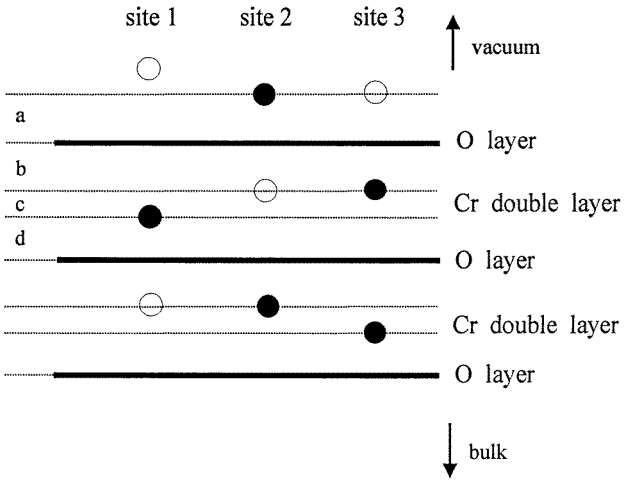

Figure 1. Sideview of the $Cr_2O_3(0001)$ surface. Occupied Cr positions are marked by full circles ●, empty positions by empty circles ○. In the relaxation models R40 and R60 the four uppermost interlayer spacings (*a*, *b*, *c*, *d*) are modified.

which have no cation directly underneath the first O layer, cf figure 1) remain at the surface, while the ions in site 1 are removed. In other words, a stable Cr-terminated $Cr_2O_3(0001)$ surface can be obtained by cutting the crystal just in the middle of the buckled Cr layer. In addition to this reconstruction, strong geometrical relaxations have been observed which reach down into the volume by four to five layers. Though there is some discrepancy concerning the amount of these interlayer relaxations [8], theoretical and experimental investigations agree that the first interlayer distance is reduced by about 50%, i.e. the Cr ions in the uppermost layer are strongly pulled toward the first O layer.

It should be mentioned that the reconstructions and relaxations of the $Cr_2O_3(0001)$ surface are rather similar to those of other oxides with corundum-type structure, e.g. $Al_2O_3(0001)$ [10–12] and $Fe_2O_3(0001)$ [13].

The experimental information about the geometrical structure of the clean and adsorbate-covered $Cr_2O_3(0001)$ surface was mainly obtained via low-energy electron diffraction (LEED), either from the LEED patterns [7] or by the analysis of the $I(V)$ curves [8]. However, these methods do not yield any information on the electronic structure. In particular, they are not sensitive to the charges of the anions or cations in the bulk or at the surface. In contrast to Al_2O_3, in the case of the transition metal oxides Cr_2O_3 and Fe_2O_3, a change of the oxidation state of the cations at the surface, e.g. a reduction from Cr^{3+} to Cr^{2+}, can also lead to a reduction of the surface charge and the surface dipole moment and might also contribute to the stabilization of the polar (0001) surface plane.

Recent electron energy-loss spectroscopy (EELS) experiments have shown that the (0001) surface of Cr_2O_3 possesses several low-lying excited states in the optical band gap, which correspond to local d–d excitations in the Cr cations [7, 14]. Due to the reduced ligand field for the Cr ions at the surface these excitations are shifted to lower energies as compared to the bulk. In [7], two rather weak loss peaks at 1.20 and 1.40 eV were assigned to electronic excitations of Cr^{3+} cations at the (0001) surface. The experimental proof that these excitations are indeed surface states was provided by the observation that they are quenched by the adsorption of CO, NO and CO_2 at the surface. A theoretical assignment was also given in [7] by means of quantum chemical *ab initio* cluster calculations, but only the unrelaxed bulk geometry was

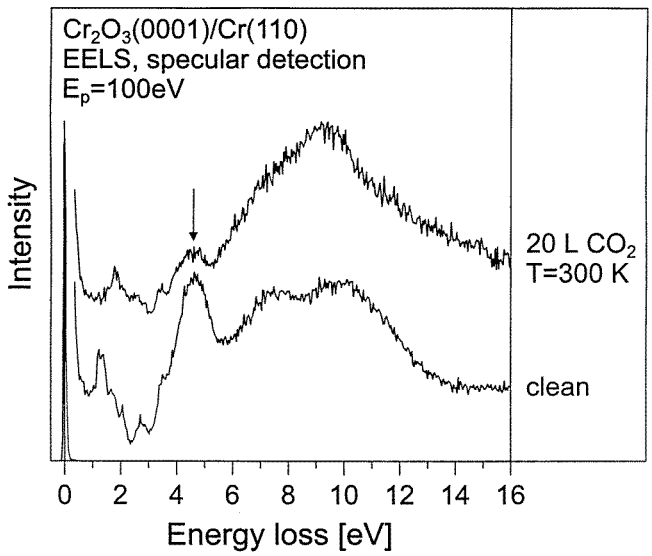

Figure 2. EEL spectra of the clean and CO_2-covered Cr_2O_3(0001) surface [14, 15].

used. An additional rather strong loss peak at 4.6 eV, i.e. also in the optical band gap, could be identified as a surface state as well [14, 15], but the nature of this excitation is still unclear. Figure 2 shows that this loss peak is strongly affected by the adsorption of CO_2; similar effects were found for the adsorption of other small molecules such as CO, NO, O_2 or Na [14, 15].

The aim of the present work is to characterize the electronic ground state as well as the low-lying excited states of the Cr_2O_3(0001) surface by means of quantum-chemical *ab initio* cluster calculations.

2. Method of calculation

Most of the present calculations were performed by means of the Bochum suite of open-shell *ab initio* programs [16–19], consisting of restricted open-shell Hartree–Fock (ROHF or SCF) [16], complete active space SCF (CASSCF) [17], valence configuration interaction (VCI) [18] and multi-configuration coupled electron pair approach (MC-CEPA) [19] programs. For some of the calculations also the GAMESS code [20] was employed.

For the Cr atom, Wachters' basis [21] was used with a (2, 1, 1, 1) contraction of the five sets of d functions; the oxygen atoms were described by Huzinaga's 9s5p basis [22], contracted to triple zeta (TZ) quality and augmented by semidiffuse s and p functions (exponents 0.1). In the H-saturated clusters, the H atoms were described by a 5s Huzinaga set [23], contracted to TZ quality as well. Several test calculations were also performed with modified basis sets, e.g. with additional polarization functions both at Cr and O, but the changes in the results are rather insignificant and are not documented in the following. The charge distribution at the various atoms has been analysed by means of the Mulliken population analysis. This allows for assigning atomic charges which, although not indicative of absolute ionicities, permit us to quantify the changes of charges and ionicities from the bulk situation to different surface relaxations.

Unless otherwise noted, the electronic excitation energies were calculated at the CASSCF level. In most calculations, the five 3d AOs of the Cr atom were included in the active space

and the orbitals were optimized for an energy expectation value averaged over the seven lowest quartet states (CASSCF 5/7).

Local properties of ionic crystals such as local electronic excitations and adsorption energies can be described quite reliably by embedded cluster models. In the present study we have chosen a cluster consisting of one metal cation and the six (for bulk Cr_2O_3) or three (for the $Cr_2O_3(0001)$ surface) adjacent O atoms. These CrO_6^{9-} or CrO_3^{3-} clusters were either saturated by protons [24] or embedded in a set of effective core potentials (ECPs) and a large array of point charges with the ionicity $+3/-2$ which simulates the Madelung potential of the extended solid. The saturation by protons was designed in such a way that either 12 (bulk Cr_2O_3) or six ($Cr_2O_3(0001)$ surface) protons were added and the Cr^{3+} ion was surrounded by neutral H_2O molecules as ligands instead of O^{2-} anions. The Cr–O distances were chosen to be 1.99 Å which is the average value of the two Cr–O distances of 1.97 and 2.02 Å in bulk Cr_2O_3 [25]. Therefore, the $[CrO_6H_{12}]^{3+}$ cluster possesses local octahedral symmetry at the Cr ion. The same Cr–O distances were also used for the $[CrO_3H_6]^{3+}$ surface cluster. Alternatively, the CrO_6^{9-} and CrO_3^{3-} clusters were surrounded by a first coordination shell of effective core potentials (ECPs) which are necessary to simulate Pauli repulsion effects and to prevent the electrons at the O^{2-} ions from flowing toward the adjacent positive charges of the embedding point charge field. Either compact model potentials [26, 27] or electron-free Na^+ pseudopotentials [28] with a charge of +3 were used for this purpose. Cluster plus ECP shell were then embedded in a large Madelung field which consisted of several thousand point charges. The calculated ionicities and excitation energies of the cluster are not sensitive to the details of the embedding point charge field. Therefore, these details are not documented here.

The cluster calculations for bulk Cr_2O_3, i.e. for $[CrO_6H_{12}]^{3+}$ or the embedded CrO_6^{9-} cluster, were performed with the ideal equilibrium geometry of bulk Cr_2O_3, both for the cluster itself as well as for the embedding point charge field. However, because of the uncertainties which still exist concerning the geometrical structure of the $Cr_2O_3(0001)$ surface, three different geometrical models for the $Cr_2O_3(0001)$ surface were considered: (i) The unrelaxed geometry with interlayer distances as in bulk Cr_2O_3; this will be called the 'ideal' geometry in the following. (ii) A geometry with relaxations of -38, -21, -25 and +11% in the first four interlayer distances relative to the unrelaxed ideal geometry. This geometry, denoted as 'R40' geometry in the following, was obtained as experimental LEED structure from the analysis of the $I(V)$ curves in [8]; however, it turned out later ([8], erratum) that an improved analysis of the $I(V)$ data leads to a new experimental LEED structure which is rather close to the geometry obtained by the MD simulations. (iii) This geometry, denoted as 'R60' geometry, with relaxations of -58, 0, -36 and +17% relative to the ideal bulk geometry, was used as a third model in the present calculations. In the two models R40 and R60 for the surface relaxation, both the geometry of the CrO_3^{3-} cluster and that of the four uppermost layers in the point charge field were modified; for the rest of the Madelung field the unrelaxed bulk geometry of Cr_2O_3 was used. Furthermore, only vertical relaxations, i.e. changes of the interlayer distances perpendicular to the (0001) surface plane, were considered since there is no experimental indication of relaxations within the O or Cr layers.

Only surface clusters with Cr ions occupying site 2 (compare figure 1) are considered in the present study. The main reason is that MD simulations [8] have shown that only site 2 is a stable position for Cr ions at the $Cr_2O_3(0001)$ surface. Sites 1 and 3 as well as the tetrahedral site are much higher in energy. They are not even local minima and they will relax towards site 2. Further, our previous calculations [7] have also shown that the local d–d excitations in the three sites (calculated with the unrelaxed bulk geometry) are very similar. Therefore, we limit our present treatment to the only stable site 2.

3. Local d–d excitations

The electronic structure of bulk Cr_2O_3 can be described as consisting of closed-shell O^{2-} ions with completely filled 2p shells and Cr^{3+} ions with the electronic configuration $3d^3$. The ground state of the metal cation in the slightly distorted octahedral environment is $^4A_{2g}$ (in O_h notation). In order to determine the ionicity of this material we have first performed ROHF calculations for the electronic ground states of the two cluster models representing the bulk situation. Table 1 shows that in the embedded CrO_6 cluster the charges at Cr and O are rather close to the formal oxidation numbers +3 and −2. The d occupation at the central Cr ion amounts to about 3.5. This means that the three t_{2g}-type 3d AOs at Cr are singly occupied each, giving rise to the $^4A_{2g}$ ground state, and about 0.5 electrons are needed to account for a small amount of covalency in the strongly ionic Cr–O bond. Though the Mulliken charges should not be taken too literally, all details of the calculations are indicative of a rather large ionicity which is best described as Cr^{3+} and O^{2-}.

Table 1. Mulliken charges and excitation energies of cluster models representing bulk Cr_2O_3[a].

	$[CrO_6H_{12}]^{3+}$	CrO_6^{9-}	Cr_2O_3 expt.
q(Cr)	2.56	2.83	
d(Cr)	3.53	3.54	
q(O)	−0.93	−2.02/ − 1.91[b]	
q(H)	0.50		
$\Delta E(^4T_{2g})$ (eV)	1.73	1.73	2.0[c], 1.8[d]
$\Delta E(^4T_{1g})$ (eV)	2.77	2.73	2.8[d]
$\Delta E(^4T_{1g})$[e] (eV)	4.44	4.43	4.1[c]

[a] q is the partial charge, in elementary charge units, at the respective atom; d(Cr) is the total occupation of the 3d AOs at Cr.
[b] Because of the difference in the Cr–O distances, the six oxygen atoms are not completely equivalent.
[c] Optical absorption data [30].
[d] EELS data [31].
[e] $^4T_{1g}$ state from ^4P of the isolated Cr^{3+} ion.

The situation is very similar in the proton-saturated cluster, the only difference being that some of the positive charge of the cluster is distributed over the terminal hydrogen atoms. In particular, the d occupation at the Cr ion is not changed as compared to the CrO_6 cluster embedded in the point charge field.

The free Cr^{3+} ion has a ^4F ground state [29]. In bulk Cr_2O_3, the sevenfold spatial degeneracy of the F state is removed by the crystal field. The new ground state is $^4A_{2g}$, the first and second excited states are $^4T_{2g}$ and $^4T_{1g}$, respectively, both also stemming from ^4F. (Since the distortion of the octahedral symmetry at the Cr^{3+} ions in bulk Cr_2O_3 and consequently also the splitting of the T_{1g} and T_{2g} states are small we have adopted the O_h symmetry notation.) The excitation energies of these states with respect to the $^4A_{2g}$ ground state are also included in table 1. They are rather similar for both cluster models and agree fairly well with optical absorption data [30] and with earlier EELS data [31]. Transitions into the lowest doublet states occur at 2.43 (^2E_g) and 2.60 ($^2T_{1g}$) eV, but they are spin forbidden and not included in table 1. The quartet state corresponding to ^4P of the free Cr^{3+} ion follows at about 4.4 eV.

The Cr ions at the (0001) surface of Cr_2O_3 are coordinated to only three O^{2-} anions and not to six as in the bulk. Therefore, the local electrostatic field at the positions of the surface Cr

Table 2. Mulliken charges in the first two layers of the $Cr_2O_3(0001)$ surface[a].

	$Cr(H_2O)_3^{3+}$	Ideal $3.0/-2.0$[d]	R40[b] $3.0/-2.0$	R60[c] $3.0/-2.0$	R60[c] $2.0/-1.667$
q(Cr)	2.33	1.97	2.01	2.09	2.12
d(Cr)	3.50	3.65	3.64	3.66	3.66
q(O)	−0.75	−1.66	−1.67	−1.70	−1.71
q(H)	0.49				

[a] q is the partial charge, in elementary charge units, at the respective atom; d(Cr) is the total occupation of the 3d AOs at Cr.
[b] 40% relaxation of the first interlayer distance (see text).
[c] 60% relaxation of the first interlayer distance (see text).
[d] The notation $3.0/-2.0$ etc indicates the values of the point charges in the first two layers of the embedding point charge field.

ions is different from the one in the bulk, and the ligand field strength, which includes covalent interactions and Pauli repulsion terms in addition to electrostatic effects, is smaller than in the bulk. Table 2 shows the response of the electronic charge distribution. Both in the hydrogen saturated CrO_3 cluster and in the embedded CrO_3 clusters with different surface relaxations, the charge at the protruding Cr ions is considerably reduced from the bulk value. The Cr atoms in the first (half occupied) Cr layer carry charges of only +2.0 instead of +3.0 in the bulk and the oxygen atoms in the next layer (i.e. in the first full O layer) only about −1.67 instead of −2.0, independent of whether the unrelaxed or the R40 or the R60 geometry is used. If the point charges in the first two layers of the embedding Madelung field are reduced to +2.0 and −1.67 the same effective charges of about +2.0 and −1.67 are recovered. (This is only documented for the R60 geometry in table 2, but the corresponding calculations for the unrelaxed and the R40 geometry show the same features.) The results in table 2 demonstrate that the properties of the CrO_3 surface cluster do not depend significantly on the embedding scheme.

Several additional calculations with modified point charge fields and with modified basis sets led to more or less the same results as those given in table 2. This also holds if the Mulliken analysis is performed for the CASSCF wavefunction for the ground state or for the lowest excited quartet states and not for the ROHF wavefunction for the ground state. In all cases, the charge at the surface Cr ion is close to +2.0 and the one at the O atoms in the first oxygen layer close to $-5/3$.

Though the ionicity of the surface Cr ions is considerably reduced as compared to the bulk, the 3d occupation remains nearly unchanged, and the ground state is still a quartet state with three singly occupied 3d AOs. A comparison of the 3d occupations given in tables 1 and 2 shows that they are increased by only about 0.1. The largest change of about 0.7 is observed in the occupation of the 4s AO. Though Mulliken charges are ill defined in cases where diffuse orbitals are to be occupied—this is the reason why we do not give explicit values for the s and p populations—there is evidence for a partial occupation of the 4s AO which is more stable for Cr ions at the (0001) surface with three neighbouring O^{2-} ions than for sixfold coordinated bulk Cr ions.

The modification of the electronic structure at the surface is also evident from the change in the lowest excitation energies of Cr_2O_3. Since the ligand field is smaller at the (0001) surface than in the bulk, the splitting of the ^{4}F state of the free Cr^{3+} ion is reduced and the excitation energies corresponding to local d $\rightarrow$ d excitations are lowered. Furthermore, since the local symmetry at the surface is reduced from O_h to C_{3v}, the degeneracy of the excited states is partly removed. The symmetry of the ground state is changed from $^4A_{2g}$ into $^4A_2$, the first excited $^4T_{2g}$ state is split into $^4A_1$ and ^4E and the next $^4T_{1g}$ state into ^4E and $^4A_2$.

Table 3. Excitation energies (in eV) and oscillator strengths of the local d → d excitations at the Cr_2O_3(0001) surface[ab].

	$Cr(H_2O)_3^{3+}$		Ideal		R40		R60	
R(Cr–O) (Å)	1.99		1.97		1.82		1.77	
X^4A_2	0.00		0.00		0.00		0.00	
1^4A_1	1.11	0.16(−4)	0.81	0.20(−5)	0.94	0.59(−6)	0.90	0.15(−5)
1^4E	1.13	0.13(−3)	1.02	0.14(−3)	1.18	0.22(−4)	1.12	0.12(−4)
2^4E	1.82	0.36(−4)	1.50	0.12(−3)	1.54	0.43(−3)	1.42	0.51(−3)
2^4A_2	2.00	0.73(−5)	1.82	0.89(−6)	1.82	0.50(−4)	1.53	0.69(−4)
3^4A_2[c]	3.32	0.27(−4)	2.55	0.12(−3)	2.80	0.19(−3)	2.98	0.18(−3)
3^4E[c]	3.58	0.56(−4)	3.59	0.23(−3)	4.13	0.53(−3)	4.21	0.63(−3)

[a] The embedding point charge fields are used with reduced ionicity (+2, −1.667) in the first two layers.
[b] The first column contains the excitation energy (in eV), the second column the oscillator strength; the notation 0.16(−4) means 0.16×10^{-4}.
[c] Components of the $^4T_{1g}$ (^4P) state.

Similarly, the $^4T_{1g}$ (^4P) state is also split into $^4A_2$ and ^4E. The transitions from the ground state into these states are optically forbidden in the undistorted octahedral symmetry, but weakly allowed at the Cr_2O_3(0001) surface.

Table 3 contains our CASSCF results for the excitation energies and oscillator strengths for $Cr(H_2O)_3^{3+}$ and the three cluster models with reduced ionicity at the surface. The corresponding results for the full surface ionicity (+3.0/ − 2.0) are so similar to those given in table 3 that they are not documented here. Table 3 shows that all excitation energies are indeed considerably lowered with respect to the bulk values (table 2) and that they are slightly increasing from the unrelaxed geometry to the R40 and R60 geometry, i.e. with decreasing Cr–O distance. The oscillator strengths are small, in particular the one for the first excited state which has $^4A_1$ symmetry and would be forbidden if the embedding point charge field had exact C_{3v} symmetry.

If dynamic correlation effects are included on top of the CASSCF calculations by means of multireference configuration interaction (MR-CI) or the multiconfiguration coupled electron pair approach (MC-CEPA) [19], the excitation energies for the lowest states (1^4A_1, 1^4E, 2^4E, 2^4A_2) change by no more than 0.03 eV, while those of the next two quartet states (3^4A_2, 3^4E) are lowered by about 0.2 eV. This can be easily explained by the fact that dynamic correlation effects are very similar for all states derived from the ^4F ground state of the free Cr^{3+} ion, while they are slightly different for the two states correlating with the excited ^4P state of Cr^{3+}.

As mentioned already in the introduction, two rather weak loss peaks at 1.2 and 1.4 eV in the EEL spectrum of Cr_2O_3 have been assigned in our previous study to electronic surface states of Cr_2O_3(0001) [7]. Our new results in table 3 confirm this assignment. The lowest excited quartet state is the optically forbidden $^4A_1$ state at 0.94 eV (R40 geometry), which is too weak to be seen in the EELS experiment. The next two states are the two weakly allowed ^4E states at 1.18 and 1.54 eV; the calculated excitation energies agree fairly well with the experimental losses. The calculations further predict both the $^4T_{2g}$ bulk state and the $^4A_2$ surface component of the $^4T_{1g}$ state in the region around 1.8 eV. This is in agreement with the experimental observation that the broad loss at about 1.8 eV is partly quenched by adsorbed molecules [7]. Similarly, at 2.8 eV one can find both the $^4T_{1g}$ (^4F) bulk state and the $^4A_2$ surface component of the $^4T_{1g}$ (^4P) state.

In our previous calculations of the local d–d excitations at the Cr_2O_3(0001) surface [7] we had hoped to be able to tell from a comparison between the observed and the calculated excitation energies which of the three possible octahedral sites is occupied by Cr ions at the (0001) surface. This was, however, not possible since we did not allow for geometry relaxations

at the surface and since the calculated excitation energies for Cr ions at the different sites were too similar to allow for a unique assignment. In the present calculations, only the most stable site, site 2 (figure 1 and [8]), was considered. This time, unfortunately, it is not possible to tell from the calculated excitation energies which relaxation model (unrelaxed, R40, R60 surface geometry) is the correct one: table 3 shows that the electronic excitation energies calculated for $Cr(H_2O)_3^{3+}$ and the three embedded surface clusters, in particular those of the two lowest ^{4}E states, differ by only 0.1–0.2 eV. This is within the range of the experimental resolution (0.15 eV [7]) as well as within the error limits of our calculations ($\sim$0.1 eV, due to basis sets, limited active space in the CASSCF calculations and point charge field). Apparently, the modification of the local crystal field at the positions of the surface Cr^{3+} ions, due to different geometric relaxations, is not strong enough to induce substantial changes in the excitation energies. Though the results for the R60 geometry, i.e. for the relaxation determined by the MD simulations and the recent LEED analysis [8], seem to fit best to the experimental EELS data [7], we cannot exclude the old LEED geometry, i.e. the R40 geometry, on the basis of the present calculations.

4. Surface charge transfer states

Figure 2 shows that in addition to the low-lying excited states with excitation energies between 1.0 and 2.8 eV there is a strong loss peak at about 4.6 eV, shortly below the onset of the charge-transfer excitations of bulk Cr_2O_3. This peak is also considerably modified by the adsorption of small molecules on the $Cr_2O_3(0001)$ surface. Weakly chemisorbed molecules such as CO or CO_2 quench the intensity of this peak to a large extent; after exposure to more reactive species like NO or O_2 it is hardly visible any longer [14, 15].

A first guess might be that this peak should be assigned to local d–d excitations from the $^4A_2$ ground state into the components of the ^{4}P state of Cr^{3+}. This state has an excitation energy of 1.74 eV in the free Cr^{3+} ion [29], but is shifted upwards by the ligand field to about 4 eV in bulk Cr_2O_3 (compare table 1). However, the transition $^4F \rightarrow {}^4P$ is optically forbidden for the free ion as is the transition $^4A_{2g} \rightarrow {}^4T_{1g}$ (^{4}P) in bulk Cr_2O_3. Therefore it can be expected that the $X^4A_2 \rightarrow 3^4A_2$, 3^4E transitions are also weak at the $Cr_2O_3(0001)$ surface. This is supported by the calculated oscillator strengths which are as small as those for the excitations within the ^{4}F manifold (table 3). Moreover, local d–d transitions should give rise to rather sharp features whereas the loss peak at 4.6 eV has a width of more than 1 eV. We therefore conclude that this peak might contain $^4A_{2g} \rightarrow {}^4T_{1g}$ (^{4}P) excitations in bulk Cr_2O_3 and at the $Cr_2O_3(0001)$ surface, but cannot be assigned exclusively to such transitions.

The second possibility is that the loss peak at 4.6 eV should be attributed to surface charge transfer excitations, i.e. to excitations in which one electron is transferred from the first full oxygen layer to the Cr^{3+} ion above the surface. It can be expected that these charge transfer excitations need less energy at the surface than in the bulk, since half of the negatively charged first coordination shell is missing for Cr ions at the surface which facilitates an electron transfer. Of course, partly occupied 3d AOs are available for the Cr ions at the surface as well as for those in the bulk.

In order to check this possibility we have performed a second series of CASSCF calculations in which one or more of the 2p AOs at the O atoms were included in the active space, in addition to the 3d AOs of the surface Cr^{3+} ion. The CASSCF optimization of the orbitals was then performed for the lowest sextet state (or an average over several low-lying sextet states) corresponding to a charge transfer excitation of the type $O2p^{-1}Cr3d^4$. (Sextet states were chosen for the CASSCF optimization since for an embedded CrO_3 cluster all local excitations have quartet or doublet spin multiplicities; sextet states are only possible for charge

transfer excitations.) These orbitals were then used for valence CI calculations in which also quartet and doublet states were included.

There are three effects which make a reliable calculation of surface charge transfer states a rather difficult task. First, charge transfer excitations generate large local dipole moments which interact quite strongly with the embedding point charge field. Therefore, the calculated excitation energies are very sensitive to the details of the embedding. In the present study, we have tried to minimize this uncertainty by using the Madelung field of Wierzbowska [32] which avoids boundary effects by choosing a unit cell without low electric multipole moments. Second, the local dipole moment will polarize the whole oxide crystal. In a cluster calculation only polarization effects within the cluster are accounted for; extracluster polarization is neglected. Therefore, the calculated excitation energies are expected to be too high [33]. Third, the orbitals optimized for the excited charge transfer states differ considerably from those optimized for the neutral ground state. Consequently, it is quite difficult to set up a valence CI, which is capable of describing local d–d excitations and charge transfer excitations equally well and obtaining reliable transition moments. We have tried to do this by increasing the number of active orbitals, but a CI with non-orthogonal orbitals [34] would be a better choice for this purpose.

Because of these difficulties, the uncertainty of the calculated excitation energies for the charge transfer states is in the order of 0.5 eV, i.e. much larger than for the local d–d excitations. The calculated transition moments are at most accurate within a factor of 2.

The CASSCF optimization places the two lowest charge transfer sextet states at excitation energies of about 3.7 eV. The charge transfer turns out to be strongly localized, that is, one electron is transferred from one O^{2-} ion to the Cr^{3+} ion at the surface, leaving one O atom with a Mulliken charge of -0.95 and the two others with charges of -1.85. Concomitantly, the d occupation at the Cr ion is increased to about 4.15. If the orbitals optimized for these sextet states are then used in a valence CI for the quartet states, one finds several charge transfer states with low intensities (small transition moments) at about 4.0–4.2 eV, and two strong transitions at 4.75 and 5.05 eV. These states have oscillator strengths of 0.012 and 0.011, respectively, i.e. about two orders of magnitude larger than those for the local d–d excitations (see table 3). The next bunch of states with large oscillator strengths follows at about 7.0 eV.

Even though the uncertainties of our numerical results for the charge transfer excitations are comparatively large, there is no doubt concerning the interpretation of the loss peaks in the EEL spectrum of Cr_2O_3(0001) in the range between 4.0 and 8.0 eV: the broad band around 4.6 eV (figure 2) consists predominantly of surface charge transfer states, in which one electron is transferred from the first oxygen layer to a Cr ion at the surface. These surface excitations have lower excitation energies than the corresponding charge transfer excitations in bulk Cr_2O_3 since the next negatively charged O layer is missing. Since large local dipole moments are generated by these excitations, the corresponding transition moments are much larger than those belonging to local d–d excitations within Cr ions.

5. Conclusions

The results of the present embedded cluster calculations for the Cr_2O_3(0001) surface can be summarized as follows.

(a) The electronic ground state is characterized by a charge distribution in which one electron is delocalized from the first oxygen layer into the 3d AOs of the Cr ions at the surface such that their ionicities are Cr^{2+} instead of Cr^{3+} in the bulk and $O^{-1.67}$ instead of O^{2-} in the bulk.

(b) Despite of this charge delocalization the Cr ions at the surface have quartet ground states with three unpaired 3d electrons.

(c) The weak loss peaks in the EEL spectrum of Cr_2O_3 at 1.2 and 1.4 eV are assigned to local d–d excitations in the Cr ions at the (0001) surface. Due to the reduced ligand field strength and lower symmetry as compared to bulk Cr_2O_3, the d–d excitation energies at 1.73 and 2.73 eV in the bulk are shifted to lower values at the surface; the spatial degeneracies of the excited states in the bulk are also partly removed.

(d) There is no substantial difference in the local d–d excitations calculated for different surface relaxations. The ligand fields at the Cr ions are strongly influenced by the coordination (sixfold coordination in the bulk, threefold at the surface), but not much modified by the different relaxations.

(e) The prominent broad loss peak at 4.6 eV in the EEL spectrum of Cr_2O_3 is assigned to surface charge transfer excitations, in which one electron is transferred from one O atom in the first oxygen layer to a surface Cr ion.

Acknowledgments

This study was financially supported by Deutsche Forschungsgemeinschaft, Ministerium für Wissenschaft und Forschung des Landes Nordrhein-Westfalen und Fonds der Chemischen Industrie. JAM benefited from a postdoctoral grant of the graduate college 'Dynamische Prozesse an Festkörperoberflächen'.

References

[1] Tasker P W 1977 *J. Phys. C: Solid State Phys.* **12** 4977
[2] Tasker P W 1979 *Phil. Mag.* A **39** 119
[3] Freund H J, Kuhlenbeck H and Staemmler V 1996 *Rep. Prog. Phys.* **59** 283
[4] Wolf D 1992 *Phys. Rev. Lett.* **68** 3315
[5] Rohr F, Wirth K, Libuda J, Cappus D, Bäumer M and Freund H J 1994 *Surf. Sci.* **315** L977
[6] Kuhlenbeck H, Xu C, Dillmann B, Haßel M, Adam B, Ehrlich D, Wohlrab S, Freund H J, Ditzinger U A, Neddermeyer H, Neuber M and Neumann M 1992 *Ber. Bunsenges. Phys. Chem.* **96** 15
[7] Bender M, Ehrlich D, Yakovkin I N, Rohr F, Bäumer M, Kuhlenbeck H, Freund H J and Staemmler V 1995 *J. Phys.: Condens. Matter* **7** 5289
[8] Rohr F, Bäumer M, Freund H J, Mejias J A, Staemmler V, Müller S, Hammer L and Heinz K 1997 *Surf. Sci.* **372** L291
Rohr F, Bäumer M, Freund H J, Mejias J A, Staemmler V, Müller S, Hammer L and Heinz K 1997 *Surf. Sci.* **389** 391 (erratum)
[9] Rehbein C, Harrison N M and Wander A 1996 *Phys. Rev.* B **54** 14 066
[10] Mackrodt W C, Davey R J, Black S N and Docherty R 1987 *J. Cryst. Growth* **80** 441
[11] Causà M, Dovesi R, Pisani C and Roetti C 1989 *Surf. Sci.* **215** 259
[12] Manassidis I, De Vita A and Gillan M J 1993 *Surf. Sci.* **285** L517
[13] Wang X G, Weiss W, Shaikhutdinov Sh K, Ritter M, Petersen M, Wagner F, Schlögl R and Scheffler M 1998 *Phys. Rev. Lett.* **81** 1038
[14] Ehrlich D 1995 *PhD Thesis* Ruhr-University Bochum
[15] Xu C, Hassel M, Kuhlenbeck H and Freund H J 1991 *Surf. Sci.* **258** 23
[16] Staemmler V 1977 *Theor. Chim. Acta* **45** 89
[17] Meier U and Staemmler V 1989 *Theor. Chim. Acta* **76** 95
[18] Wasilewski J 1989 *Int. J. Quantum Chem.* **36** 503
[19] Fink R and Staemmler V 1993 *Theor. Chim. Acta* **87** 129
[20] Schmidt M W, Baldridge K K, Boatz J A, Elbert S T, Gordon M S, Jensen J J, Koseki S, Matsunaga N, Nguyen K A, Su S, Windus T L, Dupuis M and Montgomery J A 1993 *J. Comput. Chem.* **14** 1347
[21] Wachters A J H 1970 *J. Chem. Phys.* **52** 1033
[22] Huzinaga S 1971 *Approximate Atomic Functions I* (Alberta, Canada: University of Alberta)

[23] Huzinaga S 1965 *J. Chem. Phys.* **42** 1293
[24] Pöhlchen M and Staemmler V 1992 *J. Chem. Phys.* **97** 2583
[25] Wyckoff R W G 1964 *Crystal Structures* 2nd edn, vol 2 (New York: Interscience) p 6
[26] Mejias J A and Sanz J F 1995 *J. Chem. Phys.* **102** 327
[27] Mejias J A, Oviedo J and Sanz J F 1995 *Chem. Phys.* **191** 133
[28] Fuentealba P, Preuss H, Stoll H, von Szentpály L 1982 *Chem. Phys. Lett.* **89** 418
[29] Moore C E 1971 *Atomic Energy Levels* vol I, circ. 467, NSRDS-BNS (Washington: National Bureau of Standards)
[30] Allos T I Y, Birss R R, Parker M R, Ellis E and Johnson D W 1977 *Solid State Commun.* **24** 129
[31] Kemp J P, Davis S T P and Cox P A 1989 *J. Phys.: Condens. Matter* **1** 5313
[32] Wierzbowska M 1998 private communication
[33] Janssen G J M and Nieuwpoort W C 1988 *Phys. Rev.* B **38** 3449
[34] Pykavy M and Staemmler V to be published